© Universiti Tun Hussein Onn Malaysia Publisher's Office

IJIE

http://penerbit.uthm.edu.my/ojs/index.php/ijie
ISSN : 2229-838X e-ISSN : 2600-7916

The International Journal of Integrated Engineering

Modelling and Experimental Study of Dissimilar Arc Stud Welding of AISI 304L to AISI 316L Stainless Steel

Marwan T. Mezher[1*], Osamah Sabah Barrak[2], Nasri S. M. Namer[3]

[1]Institute of Applied Arts,
Middle Technical University, Baghdad, IRAQ

[2]Institute of Technology - Baghdad,
Middle Technical University, Baghdad, IRAQ

[3]Engineering Technical College Baghdad,
Middle Technical University, Baghdad, IRAQ

*Corresponding Author

DOI: https://doi.org/10.30880/ijie.2022.14.06.009
Received 8 March 2021; Accepted 14 August 2021; Available online 10 November 2022

Abstract: This paper has aimed to try and establish a successful weld joint between AISI 304L stainless steel as a stud and AISI 316L stainless steel as a plate by using an arc stud welding process. The effect of different current and time welding on the torque results was experimentally studied, by using three-level of each process parameters. The post-weld heat treatment (PWHT) was carried out on the optimum sample of torque, to study the effect of PWHT on mechanical properties (torque and hardness) and microstructure of the welding zone. In the present work, a 3-D finite element model was developed by using ANSYS software version 18 to analyze the influence of time and current welding on the temperature distribution and residual stresses of the resultant welded joints. A transient thermal model was built to predict the temperature distribution whereas the residual stresses were determined by using a static structural model. The PWHT has been used to reduce the amount of residual stresses and enhance the mechanical properties of the welded joint. The micro-hardness based on the Vickers test and the microstructure of welded specimens of with and without PWHT have been investigated. The simulation results reveal that the generated temperature and the residual stress is strongly affected by the time and current welding. The mechanical test results indicated that the PWHT prompted an improvement in the hardness values.

Keywords: Arc stud welding, AISI304L, AISI316L, residual stress, temperature distribution, PWHT, FEM

1. Introduction

The Arc Stud Welding (ASW) is an assembling procedure that is consistently used for melts and joins studs to sheets or plates of various metals and thicknesses, wherein, the heat is moved between the stud and the plate. This welding procedure relies upon building up the heat by the electric arc that locally liquefies the contact regions of the stud and plate and physically connected them by applying a pressure in an extremely brief period. During the welding procedure happen an alteration in the mechanical properties, microstructure, and metallurgy [1-4].

The cycle of short welding is an appealing procedure in structural and automotive where productivity is the issue [5, 6]. The ASW is a process utilizing to welding of similar and dissimilar metals, the welding of dissimilar metals with aid of this process has a making significance in the light industry because of their highly practical and economical

*Corresponding author: marwantahir90@gmail.com

2022 UTHM Publisher. All rights reserved.

abilities where joining dissimilar metals can acquire a combination of their merits to optimize properties of products to match the requirements of aerospace, automobile industry, and chemical industry [7, 8]. Despite that, the welding of dissimilar metals is considered a big challenge due to the differences in physical properties and chemical composition which leads to the formation of large residual stresses and intermetallic compounds. Dissimilar welding gives the ability to pick the right metal for certain applications according to the service condition [9-12].

Dissimilar metal joining is usually fulfilled in different welding processes, where two base metals different from each other in the composition are welded together. In dissimilar metal welding, the area nearby the fusion zone usually differs significantly from the bulk weld metal in properties and composition and even in the resultant microstructure. Dissimilar metal weld joints are generally utilized in the automotive, chemical, construction, nuclear power, and petrochemical industries have given the requirement necessary form of the structure. These joints must meet with conditions of serious service that requiring good heat transfer attributes, oxidation and corrosion resistance, and high-temperature mechanical properties. Dissimilar metal weld joints with less expensive steels instead of high alloy steels make a significant investment in cost. Although the strength of the weld metal can be over composed of the base material, it is difficult to at the same time acquire good ductility, toughness, and corrosion resistance in the weldment and making the weldment resistance to failures. In this way, the right decision to choose the material is a critical issue for making dissimilar metal weld joints [13-17].

Austenitic stainless steels (ASS) are one of the broadest materials utilized in many engineering applications because they possess enhanced mechanical properties, high forming abilities, and great corrosion resistance. Consequently, these types of materials are used extensively in a variety of industrial sectors such as pharmaceuticals, food, power industries, pressure vessels, chemicals, and polymer. The similar and dissimilar welding of ASS having numerous problems in the process of welding. The dissimilar welding of ASS is a Complicated phenomenon as it can cause the find cracking and defects in the weldment. The serious problems related in the weldment products of ASS are solidification cracking, weld decay, and hot cracking, it ought to use proper filler wires with minimal impurities (S, P) to avoid the appearance of the hot cracking and solidification cracking [18-23], and use stabilized grades such as (321 & 347) and low carbon grades such as (304L & 316L) to avoid occurring the weld decay, and due to the high thermal expansion coefficient and low thermal conductivity of ASS, high residual stresses might appear in these materials after welding, consequently When they used in corrosive media, stress corrosion cracking can occur in the heat-affected zone (HAZ). Residual stress sometimes is generated in the engineering components even if there are no external forces and it is evolving foremost due to irregular volumetric variation inside the engineering parts regardless of manufacturing operations such as metal forming, casting, machining, mechanical deformation, and welding processes. A considerable amount of residual stresses is usually accompanied the different welding process affected the performance and critical integrity of parts, the mechanism of developing residual stresses in welded joints is occurring mainly due to procedures of welding process which is involved variation in the rates of heating and cooling and that is causing a non-uniform volumetric variation in expansion and contraction around the weld region. Both compressive and tensile stresses appear within the ASW joints as results of the heating and cooling respectively during the welding process.

For dissimilar welding, the determination of proper filler is exceptionally significant. The selection of improper welding parameters may cause the cracking in the weld zone and the heat-affected zone. The utilization of Ni-based filler was viewed as providing the diminishing of thermal stresses [24, 25]. N. Yazdian, et al. [26] researched about the welding of 304L stainless steel tubes utilizing dissimilar filler (A308LSi and A316LSi), They found that the filler of 316LSi reveals the excellent pitting resistance with a minimum of the region unstable passive. J. Xin, et al. [27] examined the effect of post-weld heat treatment (PWHT) on the mechanical properties and microstructure of AISI 316LN ASS. They obtained the impact toughness increment at (600 to 760) ℃ of PWHT as a result of relieving the residual stress and it drops at the higher temperature brought about by the precipitation of the brittle sigma phase. While the tensile strength is slightly reduced. A.C. Gonzaga, et al. [28] inquired about the ASS that utilized in extreme conditions, operating at the furnaces of high temperatures (500 - 675) ℃. They observed it is important to make the PWHT in the weld zone, HAZ, and BM to protect this material from the sensitization effects. H. Soltanzadeh, et al. [6] proposed a finite element modelling to analyse the resultant microstructure, temperature distribution, and residual stresses through stud weld joints. Rocha, et al. [29] performed a numerical simulation study on the influence of the cross-sectional area of the strength of the steel and the stud shanks on the stud strength. Wang, et al. [30] concluded that the residual stresses are introduced in weld joints during arc welding operations are in the self-equilibrium state due to non-uniform temperature distribution. S. H. Cho and J. W. Kim [31] pointed out the metallurgical phase transformation of medium and high carbon steel must be taken into account in the analysis of welding residual stresses. H. Dia, et al. [32] pointed out that the phase transformation change which occurs in most types of steel during the welding process has a direct influence on the welding residual stresses. Mezher et al. [33, 34] investigated numerically the influence of residual stresses on the quality of formed products through using different forming processes.

In the present study, an endeavour has been made of ASW of AISI 304L stainless steel studs to 316L stainless steel disc plates on involved three fundamental parts: the first was to explain the effects of the welding process parameters on the joint strength by an estimate of the mechanical properties before exposing them to the PWHT‘s; the second one was predestined of the influence PWHT on the mechanical properties and microstructure of the welded joints, the third

one was numerical simulation had been directed into the investigation of effect the heat source with different times of welding process on the temperature distribution and residual stresses.

2. Experimental Setup

2.1 Materials

AISI 304L of 70 mm length and 8 mm diameter is to be welded with a plate of AISI 316L by the ARC. The dimensions of the disc plate are 19 mm thickness and 28 mm in diameter, as depicted in Fig. 1. The chemical compositions and general properties of the materials are recorded in Tables 1 and 2 respectively.

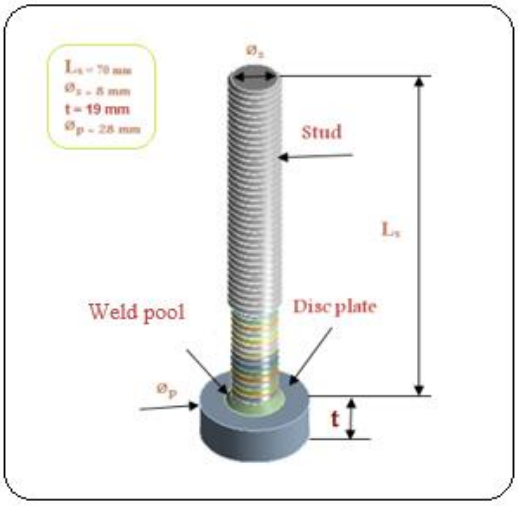

Fig. 1- Schematic of the FE model of ASW

Table 1 - Chemical composition

Element wt%	C	Si	Mn	P	S	Cr	Ni	Mo	Fe
Stud (AISI 304L)	0.025	0.7	1.63	0.03	0.01	18.7	10.4	0.2	Bal.
BM (AISI 316L)	0.023	0.62	1.59	0.029	0.018	16.6	11.1	2.2	Bal.

Table 2 - General properties

Material Property	Stud (AISI 304L)	BM (AISI 316L)
Yield Strength (MPa)	410	266
Tensile Strength (MPa)	712	647
Elongation (%)	40	38
Coefficient of thermal expansion (C^{-1})	$1.66*10^{-5}$	$1.6*10^{-5}$
Isotropic thermal conductivity ($W.M^{-1}.K^{-1)}$	16.3	15
Specific heat ($J.kg^{-1}.K^{-1}$)	500	470

2.2 Specimens Preparation

Using the ASW machine to weld the studs to sheets as illustrated in Fig. 2, the welding has been performed by employing the weld equipment parameters which represent welding current and welding time by applying three levels for each parameter, as indicated in Table 3.

Fig. 2 - The machine of ASW

Table 3 - Welding parameters of ASW

No.	Current (A)	Time (s)
1	300	0.15
2	300	0.2
3	300	0.25
4	500	0.15
5	500	0.2
6	500	0.25
7	700	0.15
8	700	0.2
9	700	0.25

2.3 Experimental Tests

The torque test was conducted on all the samples of test which are listed in Table 3, this test utilized to appraise the mechanical properties of the welding zone. Torque test was carried out according to the standard of BS EN ISO 14555:2014, by using the torque device. Upon completion the torque test and acquiring the outcomes and it investigating at that point, the optimum sample has high torque value was taken to perform the other tests depend on it, as well as to improve the mechanical properties and reduced the residual stresses of the weld joint through using the heat treatment at 630 ºC temperature and held at this temperature for (30 Min.) as a soaking time to permit complete heating of the entire part, then it will be stored in the furnace to cool down to room temperature, this procedure is known as PWHT. The Vickers microhardness test was used on the optimum sample before its heat treatment and after it to compare the effect of the heat treatment on the mechanical properties of weld metal. The Vickers microhardness test was applied by utilized the device of microhardness testing and as indicated to ASTM [35]. The hardness estimation was brought on the FZ, HAZ, and base metal (BM) by using load 300g for 15s dwell time. The microstructure examination has been carried out by using the optical microscope to investigate the microstructure of metallographic stainless steel on the optimum sample before its heat treatment and after it at three zones BM, HAZ, and FZ. It used to consider the influence of heat treatment on the types of metal grain structures. The etchant solutions were used to show the microstructure of stainless steel that; 10mL acetic acid, 10mL HNO3, 15mL HCL, and 5 drops of glycerol [36].

3. Finite Element Model

Modelling of the ASW process is considered a difficult model to simulate because of its encounter interaction between thermal (heat transfer) and mechanical phenomena. To make a verifiable prediction of residual stresses and temperature distribution during the ASW process, ANSYS (V.18) commercial software is used for that model. Simulation of heat source through this welding process is considered a big challenge, so for that, the transient thermal model has been used for the prediction of the temperature distribution during the ASW process. The heat input source is simulated according to the equations below by employing three-dimensional Goldak approach [37] which is used to predict the temperature distribution near the weld pool during welding. Moreover, Thermo-electric coupling element type was employed to mesh the model and solid element type was utilized to model the behaviour of disc plate and stud materials and the free face mesh type was used as All Quad type and the method of mesh was employed as a sweep method as clearly shown in Fig. 3. Concerning of the contact regions between the stud and disc plate and for the sake of these areas are the essential part of the current study and may be subjected an immoderate rise of the and deformation and temperature distribution throughout the proceeding welding process, consequently, a quite finer mesh with average size 0.5 mm are used for the contact regions while coarser meshes for the other parts of stud and disc which distant from contact region. The overall mesh of finite element model is composed of 14314 nodes and 31072 elements.

$$q = q_0 . e^{-3(x/x_0)2.} e^{-3(y/y_0)2} . e^{-3(z/z_0)} \quad (1)$$

$$q = \eta . \frac{6\sqrt{3}}{\pi\sqrt{\pi}} \frac{U.I.f}{z_0 y_0 x_0^2} \quad (2)$$

$$q = \eta . U . I \quad (3)$$

Where:
q: a power source (W/m^3).
(x_0, y_0, z_0): width, depth, and the outer surface dimension of the weld pool respectively.
U: Voltage drop (V).
I: Electric current (A).
η: Efficiency of welding machine.
f: Required power on the stud and plate.

Radiation and convection heat lose (q_s) to the environment occurred in the surfaces of the plate and stud is calculated by equation (4) [38]:

$$q_s = \beta (T-T_o) + \eta \xi \varepsilon (T^4-T_o^4) \quad (4)$$

Where:
β : Convection heat transfer coefficient.
T_o & T: The absolute temperature of ambient and work piece.
η : Radiation factor.
ξ : Stefan-Boltzmann constant ($5.67\times10\text{-}12$ $W/m^2 . k^4$).

Analysis of residual stresses is always considered a great concern during the ASW process, the static structural model is adopted to predict the residual stresses in the welding process and the material of the stud and plate is assumed to be a linear isotropic elasticity behaviour.

To perform a more reliable prediction of the residual stresses in the welding process, the transient model which is used for determining the temperature distribution by using the aforementioned equations and then is connected with the structural model to take into account the effect of temperature on the overall residual stresses. Through the structural model, the behaviour of the stud and disc plate materials is modelled as an isotropic homogeneous behaviour and the dimensions of the stud and disc plate in the finite element model have been taken as the same of the experimental ones.

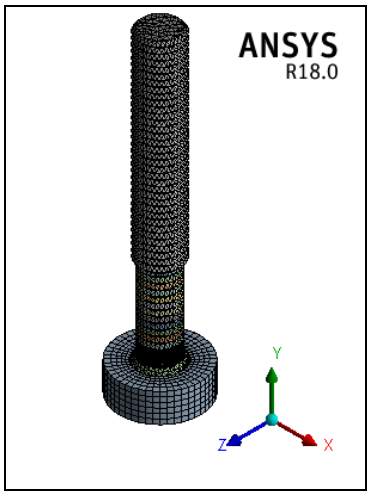

Fig. 3 - FE meshed model of ASW

4. Results and Discussions

4.1 Torque Test

Fig. 4 shows the torque test results, where the test was conducted and the findings demonstrated that the minimum torque was 25 N.M at the welding current 300A and the time 0.15 Sec, however, the maximum torque was 68 N.M which is obtained at the welding current 500A and the time 0.2 Sec, this corresponds to the specification (as indicated by the standard ISO 3506-1, 2009). For the most specimens, the failure occurred at HAZ for every sample, this indicates to acquire the greater joint strength over the picked welding parameter range. In any case, a reasonable variety in the values of torque was observed over various welding conditions. At 300A, torque value began from 25 N.M at the welding time 0.15 s and increments with expanding of welding time until arrived at peak value at 0.25 s with 44 N.M. This could be credited to adequate welding time that created a decent weld penetration and sufficient fillet around the stud [39]. When the welding current increased to 500A, the obtained torque was 68 N.M at welding time 0.2 Sec and diminished at the other welding times (0.15 and 0.25) Sec respectively, while the limit of torque when the welding current utilized 700A was 58 N.M gotten at the welding time 0.15 Sec and decreased at the other welding times. This could have come in light of the fact relatively of high heat input connected with increasing the stud melting. The variation of thermal expansion coefficient between the metals make internal stresses and influenced joint strength adversely that gives a supposition to fail under the lower torque value [40].

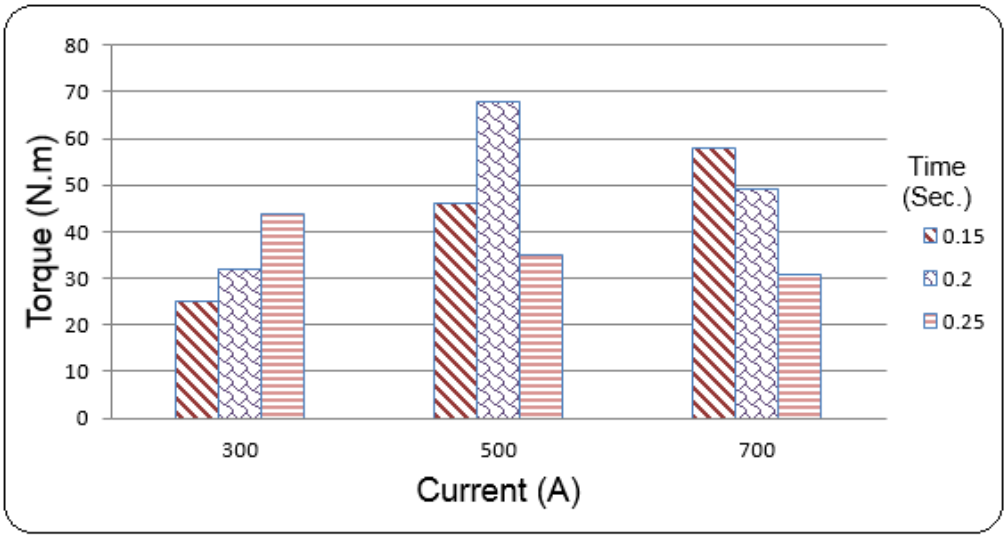

Fig. 4 - The torque values of test specimens

4.2 Post Weld Heat Treatment (PWHT)

4.2.1 Torque Test

The heat treatment was performed with the sample, which was welding parameters 500A as a welding current and 0.2 s as a welding time that is achieved the maximum torque 68 N.M, where the observed that the estimation of torque has decreased after conduct the heat treatment on the sample and reached to 56 N.M. Consequently, the PWHT attempt to diminish the mechanical properties marginally [27].

4.2.2 Microstructure

Fig. 5 shows the microstructure of metal that it has appeared the comprising of three regions were the base metal (BM), heat affected zone (HAZ), and fusion zone (FZ). The microstructure of BM as received composed of two metals, which the microstructure of AISI 316L and AISI 304L content a matrix of the grain an austenitic polygonal and a few percentages of delta ferrite. The Schaeffler formula was utilized to decide the compositions of microstructure in the HAZ and FZ by according the calculated of chromium equivalent (Cr_{eq})/ nickel equivalent (Ni_{eq}) ratio since it is observed the HAZ microstructure has differed from the microstructure of the base metal, where the microstructure in this district form of longitudinal grains close to the unaffected zone (BM) and the grains becomes acicular and globular whenever it nearby the FZ, it observed the growth of columnar dendrites along a transverse direction at the HAZ, while the FZ microstructure depicted the fine-grain comprises of austenite and expanding of percentage the delta ferrite which leads to decrease the brittleness and decrease the hardness. The microstructure of FZ shows the changes that occurred in the morphology of the austenite at dendrites and cells after welding.

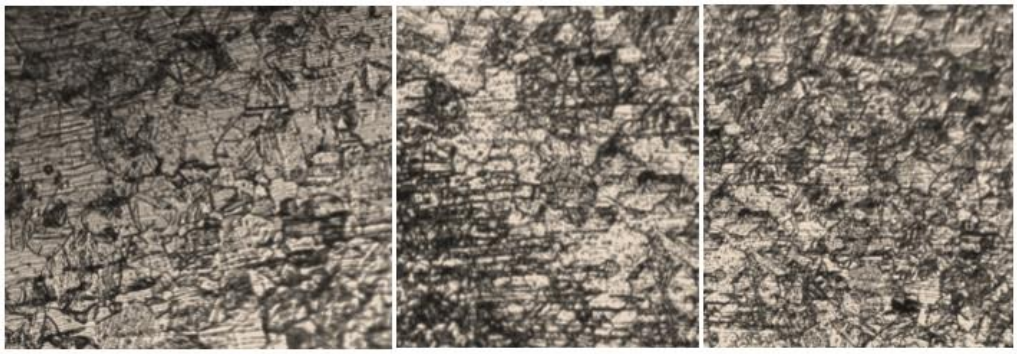

Fig. 5 - The microstructure of the optimum stud welding specimen before heat treatment

The microstructure after conducting the heat treatment of aging was indicated there is an improvement in the granular size, where it is observed the HAZ was smaller of grain size than without heat treatment. Moving toward FZ, the grain size has become fine. During the heat treatment at 630ºC, where it was occurring recrystallization and dissolution of delta ferrite at aging temperatures and the sigma phase precipitate quicker in the area of delta ferrite as their preferential locales than in regions of the austenite phase, the sigma phase found at the grain boundaries and it tends to produce a brittle phase and reduced of fracture toughness as appeared in Fig. 6. Specifically, the presence of the σ - phase, which is hard and brittle, this phenomenon is led to expanded hardness and diminished the torque so for this reason the hardness is higher compared to the metal without heat treatment.

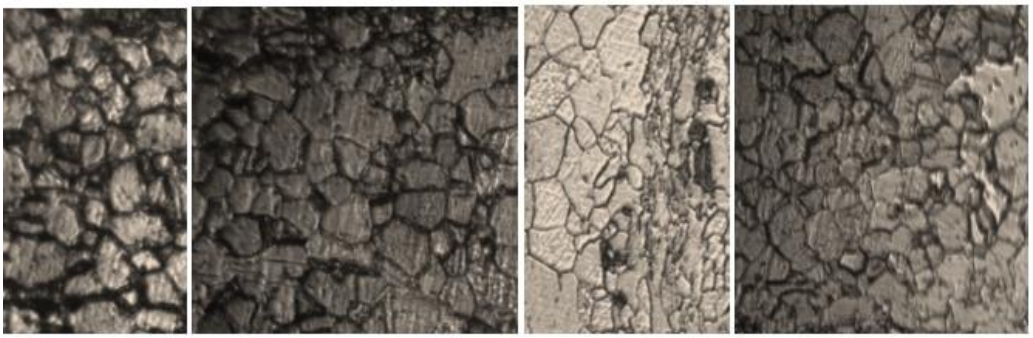

Fig. 6 - The microstructure of the optimum stud welding specimen after heat treatment

4.2.3 Hardness Test

The hardness test was conducted with the sample that is achieved the maximum torque value, through the results, it has been observed there is a variation in the amount of hardness between one region and another, where the hardness has been noted it is reached to the highest amount in the BM, but the lower value occurred at HAZ, where it is noted there is a gradual rise from the HAZ until it reaches the area that contains the FZ, which the hardness appreciative of (278 HV) and It is the same hardness value of BM (AISI 316L), but it decreases nearly 0.05% in compared with the hardness of BM (AISI 304L) as illustrated in Fig. 7.

The heat treatment was performed with the same sample after it was conducted a hardness test with it. The results appeared that it was an improvement in the amount of hardness, which it noted that the hardness reached its highest amounted to 412 HV at the region of the FZ, it increases nearly 42% in compared with the hardness of sample without PWHT as shown in Fig. 7, therefore, by comparing the hardness of with and without heat treatment, it was noticed that the heat treatment procedure exhibits higher values than the sample without heat treatment, but the hardness value at the BM remained constant. The reason for the increase of the hardness value as a result of obtaining σ-phase, which is characterized by being brittle and more hardness.

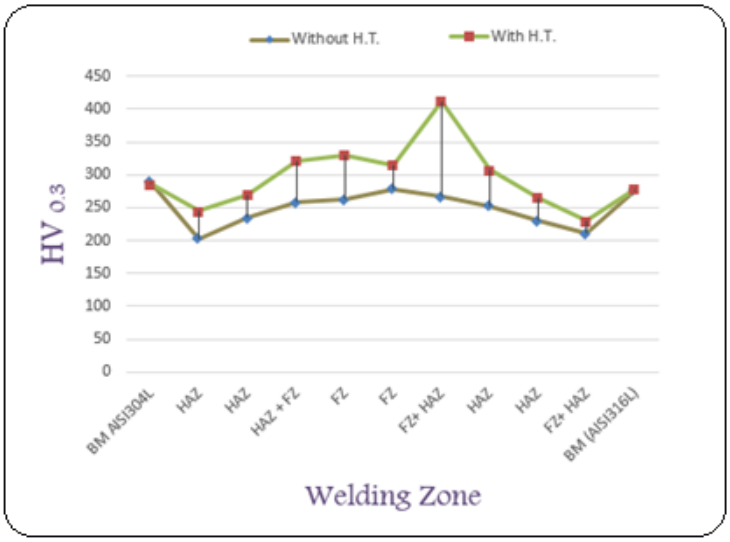

Fig. 7 - Micro hardness values of the optimum stud welding specimen with and without PWHT

4.3 Finite Element Simulation

4.3.1 Temperature Distribution

The influence of the applied current and the welding time on the temperature distribution in the region between the stud and disc plate has been investigated. It can be noticed from Fig. 8 that, the generated temperature through the ASW model is increasing with the welding time and the applied current because the generated friction force during the welding process is developed when using higher welding time. By the increasing of temperature, the vibration of atoms in the surfaces of the stud and disc plate in the contact area will increase and that leads to release theses atoms from both contact surfaces as results of breaking the bonds between them. The free atoms from both surfaces of the disc plate and the stud materials will diffuse into each other when the temperature reaches up to 1480 ºC and that leads to formation a diffusion re-join which cause the two surfaces are welded together and this is attached with results found by H. Soltanzadeh, et al. [6]. The temperature distribution in the FE model at different welding conditions is illustrated in Fig. 9.

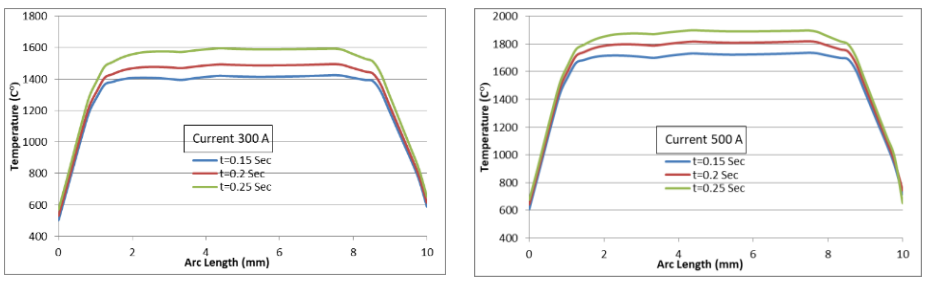

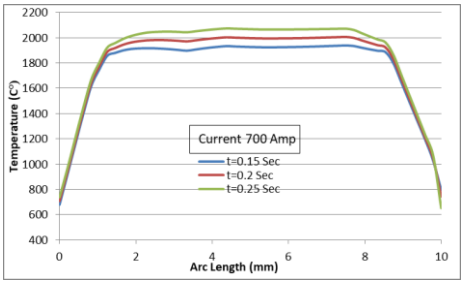

Fig. 8 - FE simulation of the temperature distribution at different welding times

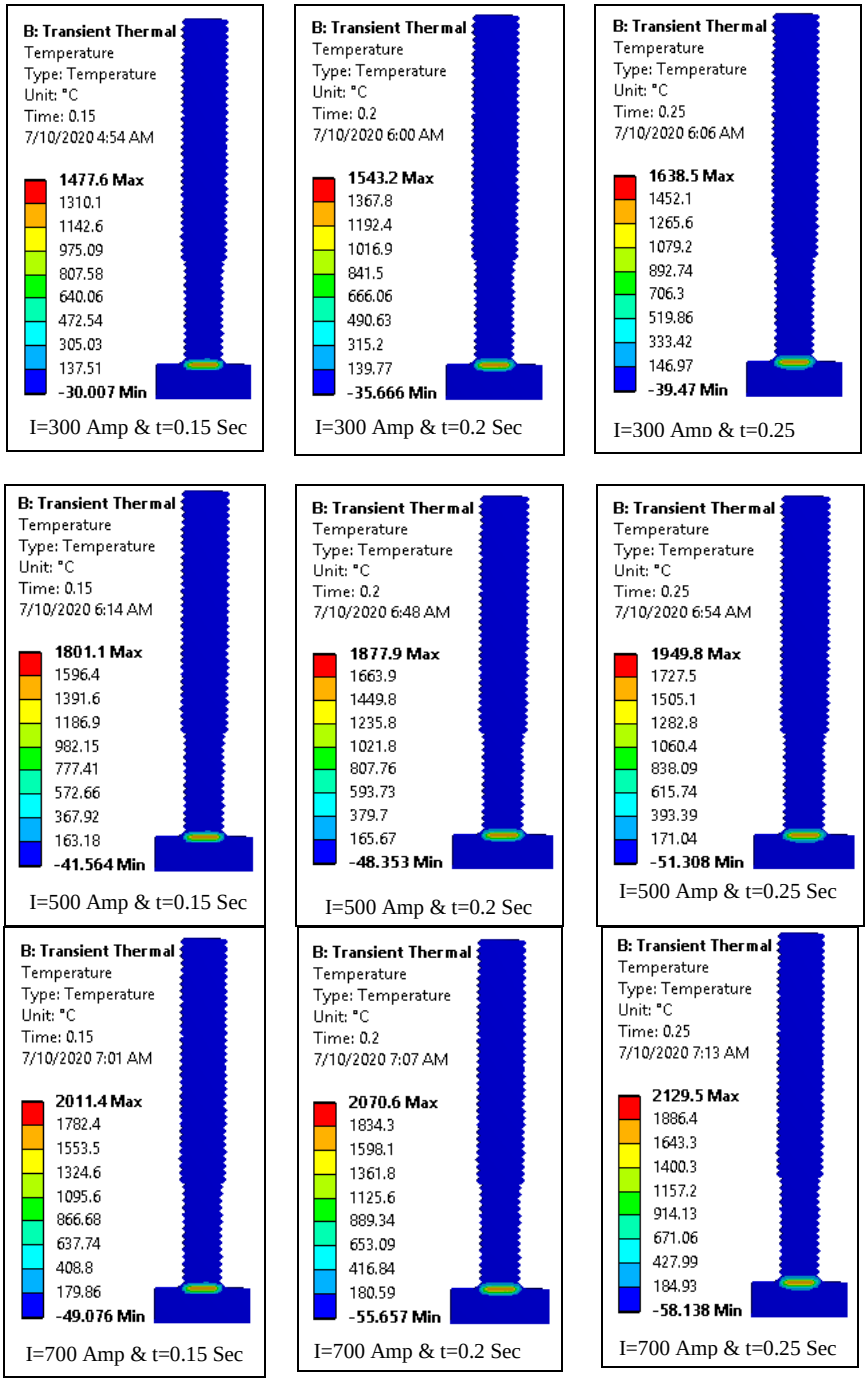

Fig. 9 - FE simulation results of temperature distribution at different welding conditions

The observations of temperature distribution over the welding specimens were homogenous for all the different conditions, the maximum generated temperature has been noticed at the centre of the contact area between the stud and the plate and it is dropped in the regions far away from the centre point during numerical simulation of the ASW process as it clearly shows in Fig. 10 for the first plate specimen.

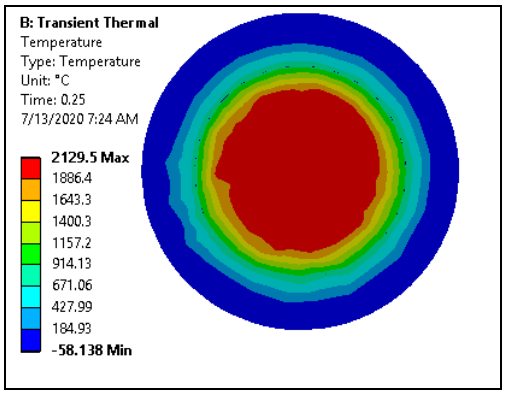

Fig. 10 - A magnified view of temperature distribution in the FE model

4.3.2 Residual stresses

The main sources of welding residual stress are solidification shrinkage, thermal contraction, quenching, and phase transformation where the tensile residual stresses own to the shrinkage while the compressive residual stresses occur due to the quenching and phase transformation.

The residual stresses in ASW simulation have been observed it is increased when the current and the time of the welding increases as shown in Fig. 11, these results were satisfied since it does not reach the elastic limit of both welding metals because if the residual stresses exceed the elastic limit that is contributing to form severe plastic deformation which is always the major cause of initiation of cracks in the welding structure.

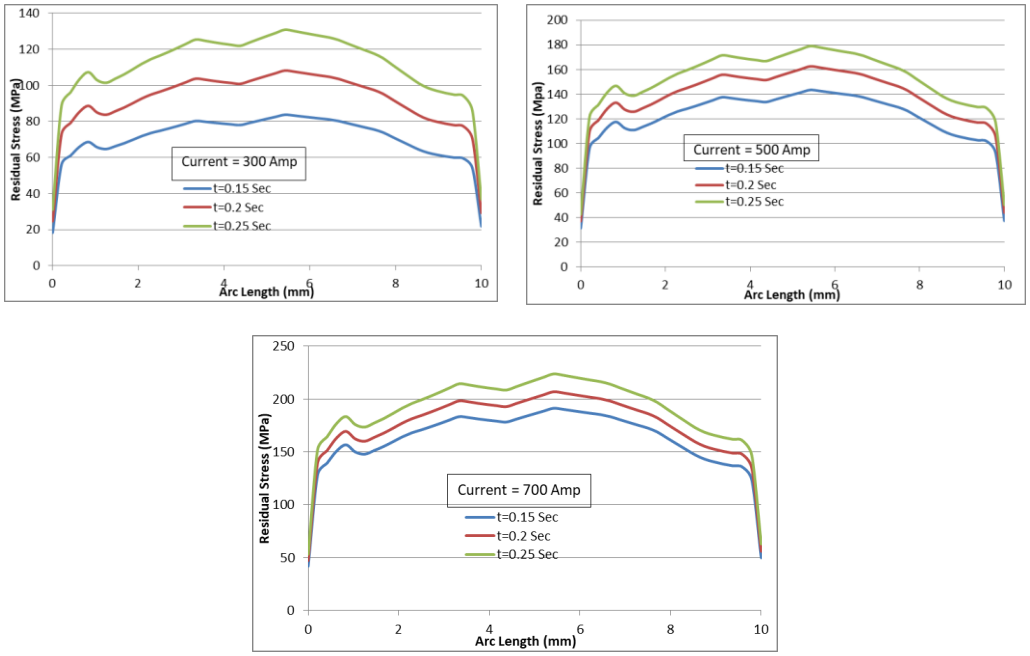

Fig. 11 - Numerical residual stresses at different welding condition

It is obvious from Fig. 12, high residual stresses were noticed in a small region of the contact area between the stud and plate and the nugget zone (NZ) exposure to the highest tensile stresses. whereas the compressive stresses are located in the region farther away from the welding area as depicted in Fig. 13.

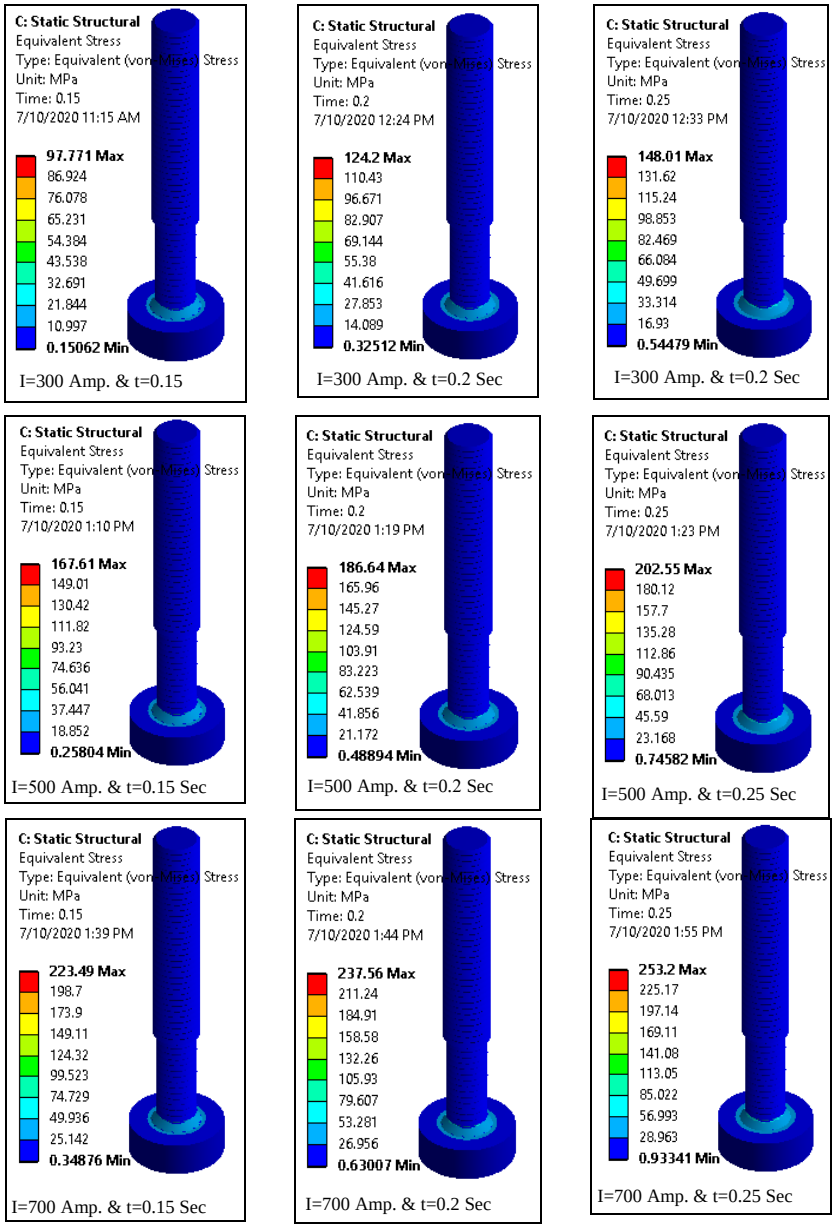

Fig. 12 - Von-Mises stress at different welding conditions

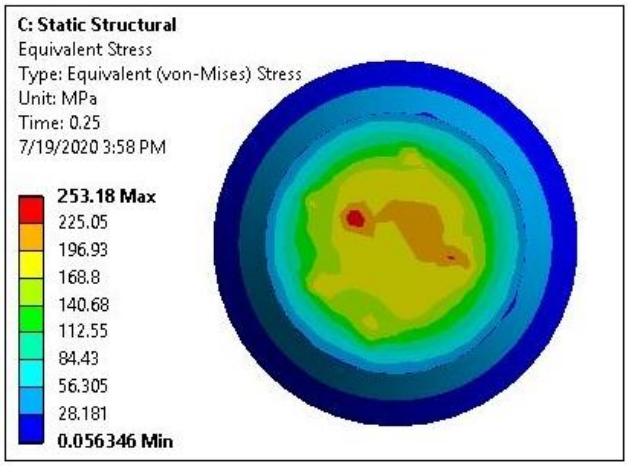

Fig. 13 - A magnified view of Von-Mises stresses in the FE model

5. Conclusions

In the current work, a numerical and experimental investigation of a dissimilar welded joint was achieved between AISI 304L stainless steel studs and AISI 316L stainless steel plate through using an ASW process. The following conclusions can be drawn from the present study:

1. The highest value of torque without PWHT was 68 N.M with the welding current 500A and the time 0.2 Sec, whereas it was 56 N.M after using PWHT at the same welding conditions.
2. The highest values of Vickers microhardness (HV) without PWHT was achieved in the BM, but the maximum value of hardness (HV) with PWHT was at the region of the FZ, and it is found increased by 42%.
3. The FE modelling by using ANSYS software show good and reliable prediction of the temperature distribution and the residual stress of the welded joints.
4. The heat input has a direct and strong effect on the temperature distribution and residual stress of the whole model.
5. The maximum ranges of temperature distribution and the residual stress have been observed at a higher time and current welding.
6. The temperature distribution was found symmetrical at the centre point of the model and reduce gradually away from the centre of the model.
7. The high residual stress was noticed in a small contact area between the stud and the plate.

Acknowledgement

Authors would like to thanks Middle Technical University that gave full support by committed technical staff to ensure all the laboratories equipments in good and functional condition.

References

[1] Fazıl Yilmaz N, Hamza A. Effect of Process Parameters on Mechanical and Microstructural Properties of Arc Stud Welds. Materials Testing. 2014;56(10):806-811.
[2] M. GB, F. MG, A. M. The Effect Arc Stud Welding Process Parameters on The Mechanical Properties of Shear Connectors in Composite Metal Deck Constructions. Journal: Structure and Steel.2014;10:16:15-23.
[3] C. Hsu, J. MUMAW. Weldability of advanced high-strength steel drawn arc stud welding. Welding journal. 2011; 90:45-53..
[4] Samardžić I, Bajić D, Klarić Š. Influence of The Activating Flux on Weld Joint Properties at Arc Stud Welding Process. Metalurgija. 2010; 49:4.
[5] C. Hsu, J. Mumaw, J. Thomas, P. Maria. Robotic stud welding process optimization with designed experiment. Welding journal. 2008; 87:10:265-272.
[6] Hadi Soltanzadeh, Jörg Hildebrand, Matthias Kraus, Mahyar Asadi. Modelling of a stud arc welding joint for temperature field, Microstructure Evolution and residual stress. In Pressure Vessels and Piping Conference. 2016-63285; V06BT06A002-9.
[7] Satoh G, Yao YL, Qiu C. Strength and microstructure of laser fusion-welded Ti-SS dissimilar material pair. Int J Adv Manuf Technol. 2013;66(1-4):469-479. https://doi.org/10.1007/s00170-012-4342-6.
[8] Chen Y, Chen S, Li L. Influence of interfacial reaction layer morphologies on crack initiation and propagation in Ti/Al joint by laser welding-brazing. Mater Des. 2010; 31:1:227-233. https://doi.org/10.1016/j.matdes.2009.06.029.
[9] M. Gholam Bargani, F. Malek Ghaini, A. Mazroi. The effect of an Al tip in arc stud welding on the properties of the welded joint. Welding Journal. 2016;95: 157-162.
[10] Barrak OS, Sar MH, Saad ML, Hussein AK, Hussein SK. Using brass foil interlayer to improve the resistance spot welding AA5451 with apply Taguchi method. J Mech Eng Res Dev. 2019;42(3):120-124.
[11] Barrak OS, Saad ML, Mezher MT, Hussein SK, Hamzah MM. Joining of Double Pre-Holed Aluminum Alloy AA6061-T6 to Polyamide PA using Hot Press Technique. IOP Conf Ser Mater Sci Eng. 2020;881(1).
[12] Başyiğit A, Kurt A. Investigation of the Weld Properties of Dissimilar S32205 Duplex Stainless Steel with AISI 304 Steel Joints Produced by Arc Stud Welding. *Metals*. 2017;7(3):77. doi:10.3390/met7030077.
[13] F. Tehovnik, B. Arzensek, B. Arh, D. Skobir, B. Pirnar, B. Zuzek. Microstructure evolution in SAF 2507 super duplex stainless steel. Mater. Technol. 2011;45(4):339-345.
[14] Abdullah, I. T., Ridha, M. H., Barrak, O. S., Hussein, S. K., & Hussein, A. K. Joining of Aa1050 sheets via two stages of friction spot technique. Journal of Mechanical Engineering Research and Developments. 2021; 44(4): 305–317

[15] Das CR, Bhaduri AK, Srinivasan G, Shankar V, Mathew S. Selection of filler wire for and effect of auto tempering on the mechanical properties of dissimilar metal joint between 403 and 304L(N) stainless steels. J Mater Process Technol. 2009;209(3):1428-1435.
[16] Mohammed Helan Sar, Osamah Sabah Barrak, Ali Shakir Al-Adili, Sabah Khammass Hussein, Abbas Khammass Hussein. Study The Effect of Filer Material on Microstructure of Welding the Carbon Steel in Shielded Metal Arc Welding. Journal of Mechanical Engineering Research & Developments (JMERD). 2020;43(3):408-416.
[17] Mezher MT, Saad ML, Barrak OS, Hussein SK, Shakir RA. Multi-coupled field simulation and experimental study of AISI 316L stainless steel using resistance spot welding. J Mech Eng Res Dev. 2021;44(2):150-160.
[18] Vashishtha H, Taiwade R V., Sharma S, Patil AP. Effect of welding processes on microstructural and mechanical properties of dissimilar weldments between conventional austenitic and high nitrogen austenitic stainless steels. J Manuf Process. 2017; 25:49-59. https://doi.org/10.1016/j.jmapro.2016.10.008.
[19] Bansod A V., Patil AP, Shukla S. Effect of heat on microstructural, mechanical and electrochemical evaluation of tungsten inert gas welding of low-nickel ASS. Anti-Corrosion Methods Mater. 2018;65(6):605-615. https://doi.org/10.1108/ACMM-05-2018-1941.
[20] Magee, J. Development of Type 204 CU Stainless, A Low-Cost Alternate to Type 304. Carpenter Technology Corporation, Reading, PA, Jan. 2001.
[21] Chuaiphan W, Srijaroenpramong L. Effect of welding speed on microstructures, mechanical properties and corrosion behavior of GTA-welded AISI 201 stainless steel sheets. J Mater Process Technol. 2014;214(2):402-408. https://doi.org/10.1016/j.jmatprotec.2013.09.025.
[22] Gurpreet Singh, Yubraj Lamichhane, Amandeep Singh Bhui, Sarabjeet Singh Sidhu, Preetkanwal Singh Bains, Prabin Mukhiya. Surface morphology and MICROHARDNESS behavior of 316L in hap-PMEDM. Facta Universitatis, Series: Mechanical Engineering. 2019;17(3):445-454. https://doi.org/10.22190/FUME190510040S.
[23] Mezher MT, Barrak OS, Nama SA, Shakir RA. Predication of Forming Limit Diagram and Spring-back during SPIF process of AA1050 and DC04 Sheet Metals. J Mech Eng Res Dev. 2021;44(1):337-345.
[24] Rahmani M, Eghlimi A, Shamanian M. Evaluation of microstructure and mechanical properties in dissimilar austenitic/super duplex stainless steel joint. J Mater Eng Perform. 2014;23(10):3745-3753. https://doi.org/10.1007/s11665-014-1136-z.
[25] Mittal R, Sidhu BS. Microstructures and mechanical properties of dissimilar T91/347H steel weldments. J Mater Process Technol. 2015; 220:76-86. https://doi.org/10.1016/j.jmatprotec.2015.01.008.
[26] Yazdian N, Mohammadpour M, Razavi R, Kovacevic R. Hybrid laser/arc welding of 304L stainless steel tubes, part 2 – Effect of filler wires on microstructure and corrosion behavior. Int J Press Vessel Pip. 2018; 163:45-54. https://doi.org/10.1016/j.ijpvp.2018.04.005.
[27] Xin J, Fang C, Song Y, Wei J, Xu S, Wu J. Effect of post weld heat treatment on the microstructure and mechanical properties of ITER-grade 316LN austenitic stainless steel weldments. Cryogenics (Guildf). 2017; 83:1-7. https://doi.org/10.1016/j.cryogenics.2017.02.001.
[28] Gonzaga AC, Barbosa C, Tavares SSM, Zeemann A, Payaõ JC. Influence of post welding heat treatments on sensitization of AISI 347 stainless steel welded joints. J Mater Res Technol. 2020;9(1):908-921. https://doi.org/10.1016/j.jmrt.2019.11.031.
[29] Bonilla Rocha JD, Arrizabalaga EM, Larrúa Quevedo R, Recarey Morfa CA. Behavior and strength of welded stud shear connectors in composite beam. *Rev Fac Ing Univ Antioquia*. 2012;(63):93-104.
[30] Wang L, Zhang QL, Chen L. Residual Stress Simulation of Stud Welding in a Rectangular Steel Tubular Surface. Appl Mech Mater. 2010;44-47:581-585. https://doi.org/10.4028/www.scientific.net/AMM.44-47.581.
[31] Cho SH, Kim JW. Analysis of residual stress in carbon steel weldment incorporating phase transformations. Sci Technol Weld Join. 2002;7(4):212-216. https://doi.org/10.1179/136217102225004257.
[32] D ai H, Francis JA, Stone HJ, Bhadeshia HKDH, Withers PJ. Characterizing phase transformations and their effects on ferritic weld residual stresses with X-rays and neutrons. In: Metallurgical and Materials Transactions A: Physical Metallurgy and Materials Science. Vol 39. Springer; 2008:3070-3078. https://doi.org/10.1007/s11661-008-9616-0.
[33] Mezher MT, Namer N, Namer NSM, Nama SA. Namer and Sami Ali Nama, Numerical and Experimental Investigation of Using Lubricant with Nano Powder Additives in Spif Process. Int J Mech Eng Technol (IJMET. 2018;9(13):968-977.
[34] Mezher MT, Saad ML, Barrak OS, Shakir RA. Finite element simulation and experimental analysis of nano powder additives effect in the deep drawing process. Int J Mech Mechatronics Eng. 2020;20(01):166-180.
[35] STANDARD, A. S. T. M. E92 2003 Standard test method for Vickers hardness of metallic materials. West Conshohocken, 2003.
[36] ASTM, E1820–05, et al. Standard test method for measurement of fracture toughness. ASTM, Annual Book of Standards, 1820, 3.
[37] Goldak J, Chakravarti A, Bibby M. A new finite element model for welding heat sources. Metall Trans B. 1984;15(2):299-305.
[38] J. P. Holman, Heat Transfer. McGraw-Hill Companies, Inc., 2010.

[39] Klarić Š., Kladarić I., Kozak D., Stoić A., Ivandić Ž., Samardžić I. The influence of the stud arc welding process parameters on the weld penetration. Scientific Bulletin Series C: Fascicle Mechanics, Tribology, Machine Manufacturing Technology. 2009;23(C):79-84.
[40] Eisazadeh H, Achuthan A, Goldak JA, Aidun DK. Effect of material properties and mechanical tensioning load on residual stress formation in GTA 304-A36 dissimilar weld. *J Mater Process Technol*. 2015; 222:344-355.